Ocean Tides for and from TOPEX/POSEIDON

C. Le Provost, A. F. Bennett, D. E. Cartwright

Comparisons of TOPEX/POSEIDON tidal solutions derived from the data of the first year of this altimetric mission with the best previous models and with in situ data show very substantial improvements. Typically, the gain in accuracy for the major lunar tidal component M_2 is 30 percent in root-mean-square differences with reference to a standard ground truth data set from 78 stations distributed over the world ocean. This is a major step, obtained because of the high quality of these altimetric data. The combination of these data with recent numerical models through assimilation methods is pointing toward solutions at the ultimate limits of practical accuracy.

Accurate information on tides is needed for many geophysical studies, such as those of the Earth's rotation and the evolution of the moon's orbit (*1*); for modern space geodesy (*2*); and for new oceanographic observation techniques such as acoustic tomography (*3*). Improved information is also needed for the study of tides themselves, especially tidal currents for computation of the horizontal flux of tidal energy, to determine where and how the dissipation of energy takes place, which is still an open question (*4*). But the most critical need now is for satellite altimetry. Satellite altimeters have been developed primarily to monitor minute changes in the slope of the ocean surface due to nontidal circulation (*5*). The tidal variation of the surface is one of the major data contaminants and must therefore be removed, with a root-mean-square (rms) accuracy of 2 cm (*6*). It is this requirement for high-quality tidal maps that has spurred scientists during the past decade to strive for better methods for analyzing the various sources of data and for modeling tides.

On 10 August 1992, the United States and France launched their joint TOPEX/POSEIDON (T/P) satellite. This mission is producing observations of the global sea surface elevation with an accuracy of 5 cm everywhere and much better accuracy over some parts of the ocean (*7*). Designed for a lifetime of 3 to 5 years, the mission is providing the ability to describe and understand the dynamics of ocean circulation and its time variability with sampling adequate to understand its climatic consequences. But the system is also working as a powerful global tide gauge. The aim of this article is to give an overview of the current status of the determination of global ocean tides and to show that T/P is now providing the most effective method for their observation.

C. Le Provost is with the Laboratoire des Ecoulements Géophysiques et Industriels, Institut de Mécanique de Grenoble, 38041 Grenoble Cedex, France. A. F. Bennett is with the Department of Oceanic and Atmospheric Sciences, Oregon State University, Corvallis, OR 97331, USA. D. E. Cartwright is Senior Research Fellow with the Institute of Oceanographic Sciences, Deacon Laboratory, Wormley, GU8 5UB, UK.

In Situ Observations

Before the era of satellite altimetry, basic information on tides came from in situ observations. Empirical charting of ocean tides from pelagic data alone is impossible because of their limited number and irregular distribution over the world ocean. But these data are vital for testing both theoretical computer-modeled and satellite-derived cotidal maps because of the very high quality of the "harmonic constants" deduced from the analysis of these time series, which are of long duration and optimally sampled. If we restrict coastal and island data to 1-year records that are less than 50 years old and on well-exposed sites, the total number of well-analyzed stations available worldwide is less than about 250. In addition, since 1965, deep pressure recorders left on the ocean floor for several months have provided truly pelagic tidal data from the open ocean (*8–10*). Such data are especially valuable for comparison because they have much less noise than do conventional surface gauges, and their harmonic constants are usually accurate, even if derived from rather short records (*11*). At present, about 350 pelagic stations have been operated, but many of them are clustered within a few hundred kilometers of the coasts of Europe and North America, which leaves large unrecorded areas in the Indian and South Pacific oceans.

Hydrodynamic Numerical Modeling

Numerical models have been developed to obtain global tidal solutions. They are based on the Laplace tidal equations, augmented by dissipation (bottom friction is the major contributor to the tidal energy budget over the continental shelves and shallow seas where tidal currents are amplified). A strong improvement in the numerical tidal models resulted from the introduction into the equations of the effects of earth tides, ocean tide loading, and self attraction. Early solutions agreed only qualitatively with in situ observations; their accuracy was not at the level required for geophysical applications, hence the need to compensate for the deficiencies of these unconstrained models by additionally forcing the solutions to fit observed data. This was the way Schwiderski got his solutions (*12*), which were considered the best available over the past decade. With a resolution of 1° by 1°, they cover the world ocean except for some semi-enclosed basins like the Mediterranean Sea. They include 11 cotidal maps: four semidiurnal $(M, S, N, K)_2$, four diurnal $(K, O, P, Q)_1$, and three long periods (Ssa, Mm, and Mf) (*13*). But the accuracy of these solutions was dependent on the quality of the observations used, and they suffered from the same weaknesses as the purely hydrodynamic models over the areas where data were not available.

In order to improve the purely hydrodynamic models, it is necessary to reproduce details of the tidal motions over the shelf areas and the marginal seas by reduction of resolution down to a few tens of kilometers. Models have been developed with grids of variable size: 4° over the deep ocean, 1° over some continental shelves, and 0.5° in particular shallow seas (*14*). Another approach uses the finite element (FE) method, which allows one to improve the modeling of rapid changes in ocean depth, the refinement of the grid in shallow waters, and the description of the irregularities of the coastlines. A FE tidal model has been implemented recently over the world ocean with a mesh size on the order of 200 km over the deep oceans, lessening to 10 km near the coasts (*15*). Pelagic and island data are used to calibrate this model, but the final runs are done without forcing the solutions to fit the data as Schwiderski did. Systematic differences from the Schwiderski solutions are noticeable; for the main tidal component M_2, they are on the order of 10 to 20 cm and even more in particular areas. When compared with the available observed data, the FE solutions are in many places closer to reality than are Schwiderski's and they offer an improved set of hydrodynamic solutions (*16*). However, discrepancies remain, partially because of uncertainties in the bathymetry.

Models with Data Assimilation

Another approach is to make a compromise satisfying the assumed dynamic equations and all the available data of good quality, treated as an inverse problem. This approach is usually known as data assimilation (*17, 18*). The best fit can be simply defined by weighted least squares. The fundamental scientific challenge is the choice of error covariances between the various data elements. Once they have been estimated, what remain are technical issues related to the computational efficiency and stability of the minimization or fitting technique. Most techniques require explicit inversion of the covariances. This inversion is a serious computational challenge. To make it feasible, one is forced to adopt oversimplified forms for the covariances. Some less direct methods, such as representer expansions (*19*), only require the use of the error covariances even though the same weighted penalty function is minimized. The representer method finds the unique solution of the Euler-Lagrange equations, which are obeyed by minima of the penalty function.

Several tentative solutions with data assimilation have been reported over the past 3 years (*18–20*). A global tidal inverse at 1° resolution with the use of equations plus data from 55 gauge stations and 15 loading gravity stations has been produced (*18*). The inversions do lead to much better agreement with data (*21*). Another application consisted of introducing a dynamic constraint in an empirical-statistical technique that had previously been successfully applied to the mapping of the M_2 tide by inversion of data from about 1200 tide gauge stations (*20*). The approach has been successfully applied to the M_2 tide mapping of the Pacific Ocean (*22*). Recently, global tidal inversions at a resolution of 0.7° by 0.7° have been done with the representer method (*19*). Careful analysis of the representer matrix allowed us to substantially reduce the number of independent variables. An inverse for K_1, with the use of pelagic and island gauge data, has given a solution grossly similar to Schwiderski's, but much smoother. All these applications demonstrate the feasibility of the assimilation approach for tidal modeling.

Altimetric Tidal Data Analysis

Satellite altimetry supplies the best data set ever obtained for studying tides globally. Although it has an unusual sampling rate and more severe error problems, a satellite altimeter operates as a huge number of open-ocean tide gauges. Data obtained globally at regular intervals of 3 to 35 days permits a clear distinction between true variations in time and geographically fixed variations such as the geoid.

Altimetry data from Seasat in 1978 first showed evidence of a tidal signal. The data were restricted by the premature termination of its 3-day repeat cycle, and analysis was only successful in limited ocean areas. Solutions in spherical harmonics have been attempted (*23*), but more physically realistic functions are available, such as normal modes (*24*) or the more primitive Proudman functions, forming a natural orthogonal basis for the dynamic equations (*25*).

The Exact Repeat Mission (ERM) of Geosat (1986 to 1989), with its 17-day repeat cycle, provided 2.5 years of altimetry data. The analysis of these data led to a plausible definition of the eight major tidal harmonics, $(M, S, N, K)_2$ and $(K, O, P, Q)_1$, in almost all ice-free ocean areas between the latitudes of ±70° (*26*). The solutions were derived by binning the Geosat observations into grid boxes 1° by 1.4754° and doing tidal analysis through a response method. The solutions were similar to those of Schwiderski, which makes empirical modeling through satellite altimetry data analysis a viable competitor for tidal definition. Empirical corrections to Geosat's computed orbit were necessary, and this was a major source of inaccuracy in the Geosat tidal solutions.

In order to diagnose the accuracy of the available tide solutions before T/P, a set of

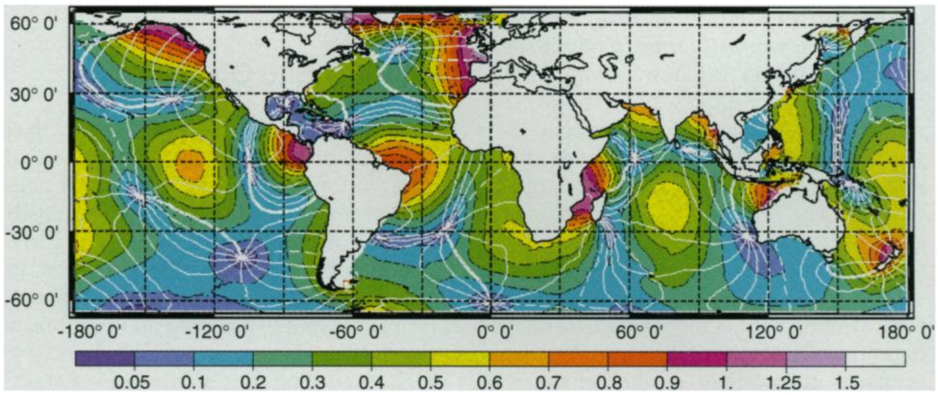

Fig. 1. Cotidal maps of the M_2 component issued from the empirical analysis of 1 year of T/P data. This solution is from Schrama and Ray (*28*). Co-amplitude lines are drawn following the color scaling indicated under the map; units are in centimeters. Co-phase lines are drawn with an interval of 30°, with the 0° phase as a thicker line, referred to the passage of the M_2 astronomical forcing at the Greenwich Meridian.

Table 1. Comparison of tidal solutions. Root mean square differences with a standard ground truth data set from 78 stations distributed over the world ocean (numbers are in centimeters).

	M_2	S_2	O_1	K_1	Total rms
Range	59	18	12	22	—
Cartwright and Ray (*26*)	3.72	2.63	1.33	1.96	5.13
Le Provost *et al.* (*15*)	3.36	1.86	1.34	1.41	4.31
Schrama and Ray (*28*)	2.42	1.69	1.27	1.50	3.55
Egbert *et al.* (*19*)	2.75	1.65	1.25	1.61	3.80

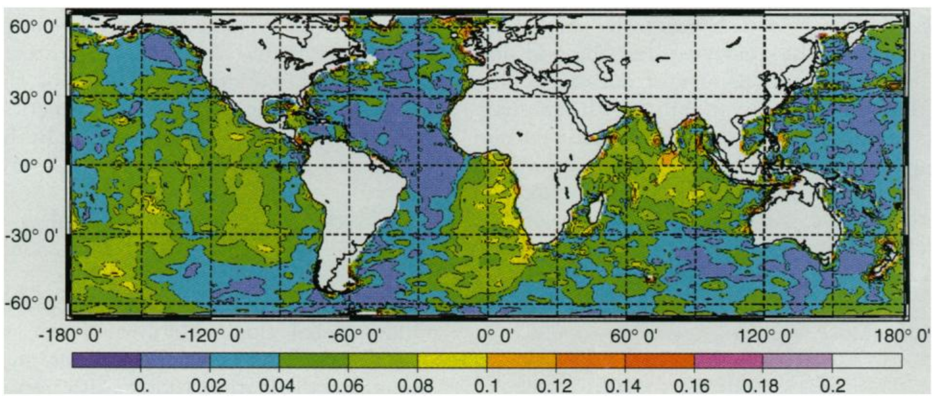

Fig. 2. Differences between the Geosat altimeter-derived M_2 solution of Cartwright and Ray (*26*) and the T/P empirically derived solution of Schrama and Ray (*28*). Scales are in centimeters.

78 pelagic and island stations was selected for comparison. For the altimetric solutions, special allowance has to be made for the load tide of the solid Earth, which is included in the geocentric tide sensed by the altimeter but not in conventional ocean tide measurements. The rms differences with the in situ data set of the solutions of Cartwright and Ray and those of Le Provost and colleagues are given in Table 1. These differences are about 6% of the mean range for the major lunar tide M_2 and between 6 and 10% for the other constituents. The two sets of solutions are at the same level of accuracy for the lunar tides M_2 and O_1, and the Geosat solution is somewhat inferior for the solar tides S_2 and K_1 (*26*). The M_2 and O_1 FE solutions are effectively close to the Geosat solutions (*15*). They agree within a few centimeters in absolute difference (less than 6 cm for M_2) over large parts of the ocean. Short-scale discrepancies are due to variable signal-noise ratio in the altimeter data (*27*). The differences at larger scales, going up to 10 to 12 cm locally, are due, on one hand, to the empirical correction applied to the Geosat satellite orbit in the altimetry solution (*28*) and, on the other, to inaccuracies in some of the parameters of the FE model (*15*). Although still imperfect, these last two solutions were considered the best available before the new T/P solutions were produced.

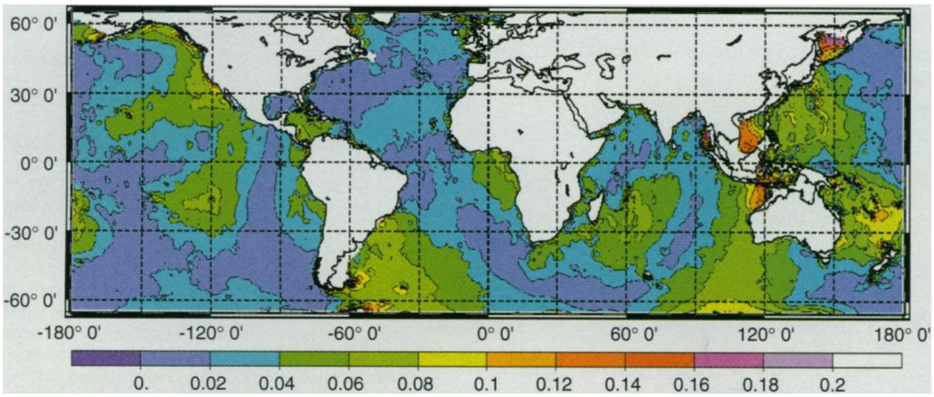

Fig. 3. Differences between the numerically computed M_2 solution of Le Provost *et al.* (*15*), and the T/P empirically derived solution of Schrama and Ray (*28*). Scales are in centimeters.

Table 2. Tidal aliasing periods of the eight major ocean tide constituents for the last three satellite altimetry missions.

Tidal component	Tidal period (hours)	Aliased period (days)		
		Geosat (17 days)	ERS1 (35 days)	T/P (10 days)
M_2	12.42	317	95	62
S_2	12.00	169	∞	59
N_2	12.67	52	97	50
K_2	11.97	88	183	87
K_1	23.93	176	365	173
O_1	25.82	113	75	46
P_1	24.07	4466	365	89
Q_1	26.87	74	133	69

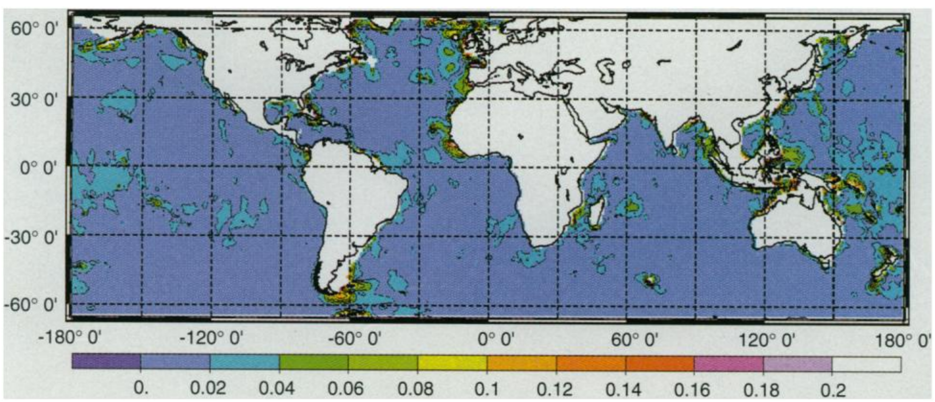

Fig. 4. Differences between the M_2 solution issued from the assimilation of 1 year of T/P data, from Egbert *et al.* (*19*), and the T/P empirically derived solution of Schrama and Ray (*28*). Scales are in centimeters.

Results from T/P

The T/P mission (*7*) provided two major improvements in satellite altimetry for tidal analysis. The first improvement results from the satellite's orbital configuration (66° inclination, 1336-km altitude, and 9.916-day repeat period), chosen so that tidal aliases are well removed from expected oceanographic signals. Table 2 lists the tidal aliasing periods for the eight major ocean tide constituents, for Geosat (17-day repeat orbit), European Remote Sensing satellite 1 (ERS1) (35-day repeat orbit), and T/P (10-day repeat orbit). T/P is the best of the three satellites for tidal mapping: The alias periods are 62 days for M_2, 59 days for S_2, and 50 days for N_2; the longest aliased period is 173 days for K_1. However, several of these aliased periods are close, so that the separation of the corresponding components requires theoretically quite long series of observation—nearly 3 years to separate M_2 and S_2. These are not yet available. The second improvement is that the error budget is lower than for any earlier mission.

After only 1 year of data collection, the application of the different methods presented above has already produced improved tidal solutions. Even the simpler empirical methods, based on direct Fourier analysis (*28*) or using admittance (*29*), have been successfully applied. To overcome the aliasing constraints, which are particularly severe for these direct approaches with only 1 year of measurements, it has been necessary to bin the data on quite large grid boxes of several degrees in order to sample a wider range of phases. These empirical methods lead thus to solutions on coarse grids, proposed as corrections to the existing tidal models. Figure 1 shows a map of the solution of the principal lunar tide M_2 derived from an empirical analysis of 1 year of T/P data (*28*), which corresponds to the best score in Table 1. Figure 2 shows the differences between this empirically produced T/P M_2 solution (*28*) and the Geosat derived solution (*26*), and Fig. 3 shows the differences with the FE solution (*15*). These figures clearly illustrate the convergence of the tidal solutions: The dark blue areas (less than 2-cm difference) cover very large parts of the global ocean. The T/P derived solutions are the closer to reality; reference to the ground truth test is the most convincing way to illustrate the gain in accuracy obtained with the new T/P solutions (see Table 1). An improvement of almost 1 cm—that is, 30%—in rms difference is observed for the M_2 tide between the FE solution (3.36 cm) and the empirically derived T/P solution (2.42 cm) (*30*).

The T/P empirically derived solutions rely heavily on averaging of the data over areas of about a 3° radius, which is necessary to overcome the tidal aliasing constraints. Indeed, a detailed analysis of these solutions reveals that they are a little noisy, spatially. Their accuracy is also limited over areas where tides are spatially complex. One way to reduce these limitations is to use the more sophisticated methods developed and tested before the advent of T/P (see preceding sections). An application has been realized successfully on the basis of the representer method, assimilating most of the cross-over data from 38 T/P cycles (*19*). An inverse solution has been computed on a 0.7° by 0.7° grid for a direct determination of the four principal tidal constituents M_2, S_2, K_1, and O_1 (*31*). These solutions are computed totally independently of any previously known tidal solution. By reference to the previous non-T/P solutions, the inverse solutions reduce the misfits for all the constituents except K_1 (see Table 1). They differ from the empirical T/P solutions by only a few centimeters (see Fig. 4), but the assimilated solutions are much smoother. Analysis of the differences from pelagic data reveals that the largest discrepancies occur at equatorial latitudes. This could be due to limitations of the 1-year data set used for these preliminary analyses. This applies particularly to the K_1 component, which is the only one in the T/P aliased spectrum to have a large aliased period—173 days.

Conclusions

With longer T/P observations, signal-noise ratio will be improved and aliasing problems will be removed. It is expected that the above numbers will be reduced again by a factor of 1.4 to 1.5, which approaches the limits of tidal analysis methods (*32, 33*). The combination of high-quality altimetry and increases in computer resources (making it possible to increase the physical realism and the resolution of the numerical models) all point toward further improvements in tide modeling in the next few years. There is a strong probability of a model of 2- to 3-cm rms accuracy, at least in the deep ocean areas, being made available soon. This is the limit of practical precision (*32*). These tidal solutions will benefit many fields of geodesy, geophysics, oceanography, and space technology. They will also supply barotropic tidal currents in the deep ocean and shallow seas, with high resolution over continental shelves, owing to the new hydrodynamic models. Thus, they will also benefit environmental and engineering investigations along coasts and marginal seas.

REFERENCES AND NOTES

1. R. D. Ray, D. J. Steinberg, B. F. Chao, D. E. Cartwright, *Science* **264**, 830 (1994).
2. D. D. McCarthy, *IERS Standards* (IERS Technical Note No. 13, Observatoire de Paris, Paris, 1992), chap. 7–10.
3. R. H. Hendrick, J. L. Spiesberger, P. J. Bushong, *J. Acoust. Soc. Am.* **93**, 790 (1993).
4. D. E. Cartwright and R. D. Ray, *Geophys. Res. Lett.* **16**, 73 (1989).
5. C. Wunsch and E. M. Gaposchkin, *Rev. Geophys. Space Phys.* **18**, 725 (1980).
6. C. J. Koblinsky, P. Gaspar, G. Lagerloef, *The Future of Spaceborne Altimetry: Oceans and Climate Change* (Joint Oceanographic Institutions, Washington, DC, 1992).
7. L. L. Fu *et al.*, *J. Geophys. Res.* **99**, 24369 (1994).
8. F. E. Snodgrass, *Science* **162**, 78 (1968).
9. J. H. Filloux, *J. Phys. Oceanogr.* **10**, 1959 (1980).
10. D. E. Cartwright, A. C. Edden, R. Spencer, J. M. Vassie, *Philos. Trans. R. Soc. London Ser. A* **298**, 87 (1980).
11. Analyses of pelagic records in the northeastern Pacific and the Southern Ocean suggest that background variances in the combined semidiurnal and diurnal bands are about 1 to 4 cm^2.
12. E. W. Schwiderski, *Mar. Geod.* **6**, 219 (1983).
13. There is a tradition of giving names to the most important frequencies present in the tidal signals. These names were given in Darwin's scientific papers [(Cambridge Univ. Press, Cambridge, 1907), vol. 1, p. 5]. As an example, the 2 cycles per lunar day and 2 cycles per solar day frequencies are called M_2 and S_2.
14. J. Krohn, *Mar. Geophys. Res.* **7**, 231 (1984).
15. C. Le Provost, M. L. Genco, F. Lyard, P. Vincent, P. Canceil, *J. Geophys. Res.* **99**, 24777 (1994).
16. These solutions are available at an anonymous ftp site (meolipc.img.fr, pub/CDROM).
17. A. F. Bennett and P. C. McIntosh, *J. Phys. Oceanogr.* **12**, 1004 (1982).
18. W. Zahel, *J. Geophys. Res.* **96**, 20379 (1991).
19. G. D. Egbert, A. F. Bennett, M. G. G. Foreman, *ibid.* **99**, 24821 (1994).
20. F. Jourdin, O. Francis, P. Vincent, P. Mazzega, *ibid.* **96**, 20267 (1991).
21. In this application, the size of the problem is reduced by the imposition of exact conservation of mass, elevation being then a dependent variable. An iterative method with a simple preconditioning is applied.
22. This dynamic constraint was based on the above-mentioned FE hydrodynamic model (*15*), and the minimization function was computed on the associated finite elements; this choice has the practical advantage of fixing the dimension of the problem.
23. P. Mazzega, *Nature* **302**, 514 (1983).
24. P. L. Woodworth and D. E. Cartwright, *Geophys. J. R. Astron. Soc.* **84**, 227 (1986).
25. B. V. Sanchez and D. E. Cartwright, *Mar. Geodesy* **12**, 81 (1988).
26. D. E. Cartwright and R. D. Ray, *J. Geophys. Res.* **96**, 16897 (1991).
27. M. G. Schlax and D. B. Chelton, *ibid.* **99**, 12603 (1993).
28. E. J. O. Schrama and R. D. Ray, *ibid.*, p. 24799.
29. X. C. Ma, C. K. Shum, R. J. Eanes, B. D. Tapley, *ibid.*, p. 24809.
30. This gain is significant if we refer to the statistical test of Fisher-Snedecor. With 156 values (real and imaginary parts of the differences from the 78 sea truth data), this test states that two rms values are significantly different if the ratio of their variance is larger than 1.32. These T/P-derived empirical solutions are available at anonymous ftp sites geodesy.gsfc.nasa.gov, dist/ejo for (*28*) and csr.utexas.edu, pub/tide for (*29*).
31. These solutions are available at an anonymous ftp site (oce.orst.edu, /pub/tides).
32. J. M. Molines *et al.*, in preparation.
33. With longer T/P time series, it will be also easier to extract the semimonthly and monthly tidal constituents. The amplitudes of these components are non-negligible. New solutions are awaited to show how far these long-period tides differ from the equilibrium form. See D. E. Cartwright and R. D. Ray, *Geophys. Res. Lett.* **17**, 619 (1990).

34. Material for this paper was provided by a number of investigators associated with the T/P Science Team and cited in the text. This article was written on the behalf of the T/P Tide Group. The T/P Science Working Team is supported jointly by the U.S. National Aeronautics and Space Administration and by the French Centre National d'Etudes Spatiales. Results reported here were obtained by the different teams of the T/P Tide Group, supported by their national authorities. These results are primarily a consequence of the exceptional quality of the mission, thanks to the work of the T/P project staff.